

Washington University School of Medicine

Digital Commons@Becker

2020-Current year OA Pubs

Open Access Publications

9-1-2022

Disease burden affects aging brain function

Lori L Beason-Held

Danielle Fournier

Andrea T Shafer

Elisa Fabbri

Yang An

See next page for additional authors

Follow this and additional works at: https://digitalcommons.wustl.edu/oa_4



Part of the [Medicine and Health Sciences Commons](#)

Authors

Lori L Beason-Held, Danielle Fournier, Andrea T Shafer, Elisa Fabbri, Yang An, Chiung-Wei Huang, Murat Bilgel, Dean F Wong, Luigi Ferrucci, and Susan M Resnick

Research Article

Disease Burden Affects Aging Brain Function

Lori L. Beason-Held, PhD,^{1,*} Danielle Fournier, PhD,¹ Andrea T. Shafer, PhD,¹ Elisa Fabbri, MD,¹ Yang An, MS,¹ Chiung-Wei Huang, MS,¹ Murat Bilgel, PhD,¹ Dean F. Wong, MD,² Luigi Ferrucci, MD, PhD,¹ and Susan M. Resnick, PhD¹

¹Intramural Research Program, National Institute on Aging, NIH, Baltimore, Maryland, USA. ²Department of Radiology, Washington University School of Medicine, St. Louis, Missouri, USA.

*Address correspondence to: Lori L. Beason-Held, PhD, Intramural Research Program, National Institute on Aging, NIH, 251 Bayview Blvd., Baltimore, MD 21224-6825, USA. E-mail: heldlo@mail.nih.gov

Received: April 7, 2021; Editorial Decision Date: July 19, 2021

Decision Editor: Lewis Lipsitz, MD, FGSA

Abstract

Background: Most older adults live with multiple chronic disease conditions, yet the effect of multiple diseases on brain function remains unclear.

Methods: We examine the relationship between disease multimorbidity and brain activity using regional cerebral blood flow (rCBF) ¹⁵O-water PET scans from 97 cognitively normal participants (mean baseline age 76.5) in the Baltimore Longitudinal Study of Aging (BLSA). Multimorbidity index scores, generated from the presence of 13 health conditions, were correlated with PET data at baseline and in longitudinal change ($n = 74$) over 5.05 (2.74 SD) years.

Results: At baseline, voxel-based analysis showed that higher multimorbidity scores were associated with lower relative activity in orbitofrontal, superior frontal, temporal pole and parahippocampal regions, and greater activity in lateral temporal, occipital, and cerebellar regions. Examination of the individual health conditions comprising the index score showed hypertension and chronic kidney disease individually contributed to the overall multimorbidity pattern of altered activity. Longitudinally, both increases and decreases in activity were seen in relation to increasing multimorbidity over time. These associations were identified in orbitofrontal, lateral temporal, brainstem, and cerebellar areas.

Conclusion: Together, these results show that greater multimorbidity is associated with widespread areas of altered brain activity, supporting a link between health and changes in aging brain function.

Keywords: Brain activity, Health, Imaging, MRI, PET

Age is a primary risk factor for a myriad of health-related medical conditions (1). In fact, it is estimated that up to 80% of people in the United States over the age of 65 have more than one serious medical condition (2). Of those individuals, 23% have conditions significant enough to be considered in poor health, meaning that illness impacts activities of daily living and often results in an overall lower quality of life (3). Age is also the primary risk factor for cognitive decline and dementia (4,5), highlighting a link between health status and the development of cognitive impairment in older individuals.

Over the past several years, studies have investigated the link between the number of medical conditions an individual has, known as multimorbidity, and the development and progression of dementia. These studies have shown that multimorbidity is a predictor for mild cognitive impairment (MCI) (6,7) or the prodromal stage of

Alzheimer's disease (AD), and that health factors most associated with MCI are hypertension and other vascular-related conditions (7,8). Further studies have shown that multimorbidity is associated with progression from MCI to AD (9), with greater multimorbidity linked to more rapid cognitive decline and progression of dementia severity (10,11). On a more practical level, physicians, and especially geriatricians, often report that patients with substantial multimorbidity frequently develop cognitive problems, and that effective treatment of non-neurological health conditions tends to improve cognitive function. However, this observation has not been fully investigated and the mechanisms that connect brain health with multimorbidity remain unclear.

Although few have investigated the impact of multimorbidity on the brain, two studies point to a link between multimorbidity

and brain structure and function. Using a large sample of cognitively normal older participants from the Mayo Clinic Study of Aging (MCSA), Vassilaki and colleagues (12) found that increased multimorbidity is associated with alterations in cortical thickness and glucose metabolism in regions of known AD pathology. Data from the Dallas Heart Study also show older individuals with medical comorbidities have accelerated increases in white matter (WM) hyperintensity volume with increasing age (13). These findings suggest that multimorbidity may influence brain structure and function, particularly in regions vulnerable to neuropathologic changes in AD.

Whereas previous studies have examined brain structure or function within predefined regions, we examine the relationship between multimorbidity and brain function in the Baltimore Longitudinal Study of Aging (BLSA) using a whole brain voxel-level technique. Annual resting-state ^{15}O -water positron emission tomography (PET) scans were used to assess regional cerebral blood flow (rCBF) as an index of brain function (14). Brain activity measured by ^{15}O -water PET is based on the principle that local increases in neuronal activity lead to co-localized regional increases in blood flow to meet the increased glucose and oxygen demand of the activated tissue (15). In this way, rCBF is an indirect measure of localized neuronal activity.

In this study, we examined the cross-sectional and longitudinal relationships between multimorbidity and brain function in a group of 97 cognitively normal older participants in the Baltimore Longitudinal Study of Aging (BLSA). We generated multimorbidity index scores based on the number of the following 13 conditions each person exhibited: anemia, cancer, congestive heart failure, chronic kidney disease (CKD), chronic obstructive pulmonary disease (COPD), diabetes, hip fracture, heart ischemic disease, hypertension, joint disease, Parkinson's disease, peripheral artery disease, and subclinical stroke/transient ischemic attack (TIA) (16). The relationship between multimorbidity score and baseline rCBF was examined, as well as the relationship between change in multimorbidity score over time and longitudinal change in rCBF.

Method

Participants

The BLSA is a study of natural human aging established in 1958 and conducted by the National Institute on Aging (NIA) Intramural Research Program. The BLSA continuously enrolls healthy volunteers aged 20 years and older who are followed for life to assess changes in health and functional status (17). We used data from 97 cognitively normal older participants (>50 years of age at baseline; 50 males; mean age 76.5 (7.8 SD)) from the neuroimaging substudy of the BLSA who had concurrent assessment of multimorbidity and ^{15}O -water rCBF PET scan collected on a GE Advance scanner at baseline (Table 1). Of these 97 participants, 74 had annual concurrent multimorbidity and longitudinal PET assessments collected over a period of 5.05 (2.74) years. None of the individuals in this study had a clinical diagnosis of mild cognitive impairment or dementia throughout the study interval. The individuals were also free of significant health conditions that could affect brain function (ie, clinical stroke with brain tissue loss or displacement, closed head injury, brain surgery, malignant cancer, meningiomas and cysts with brain tissue displacement, seizure, and bipolar disorders).

This study was approved by the local Institutional Review Boards. All participants provided written informed consent prior to each assessment.

Table 1. Participant Demographics

Participants (<i>n</i>)	97
Males, <i>n</i> (%)	50 (51.5%)
Age (years)	76.5 (7.8)
Scan Interval (mean years [SD]; <i>n</i> = 75)	5.05 (2.74)
Baseline MMSE (mean years [SD])	29.1 (1.0)
Baseline Multimorbidity Index Score (mean [SD])	2.86 (1.63)
Baseline Multimorbidity Index Range	0–7
Last Visit Multimorbidity Index Score (mean [SD])	3.24 (1.79)
Last Visit Multimorbidity Index Range	0–7

Note: Mini-mental State Exam (MMSE) score out of a possible 30. Multimorbidity Index represents the average number of disease conditions.

Multimorbidity Index

The multimorbidity index was defined at the baseline visit (ie, first concurrent assessment of multimorbidity and ^{15}O -water PET) and at each longitudinal assessment. It was defined as the number of diagnosed conditions from a predefined list of 13 conditions. These conditions were chosen based on the high prevalence and high risk of disability in older adults, the availability of adjudicated data in the BLSA database, and the use of these conditions in previous studies of BLSA participants (18,19). Hypertension, diabetes, ischemic heart disease, congestive heart failure, COPD, cancer, Parkinson's disease, hip fracture, and lower extremity joint disease were defined using standard criteria that combined information from self-reported medical history, medication use, medical documents, and a clinical medical examination. Anemia was defined as hemoglobin <12 g/dL in women and <13 g/dL in men; CKD was defined as glomerular filtration rate estimated using the Cockcroft–Gault equation <30 mL/L, and peripheral arterial disease was defined as ankle-brachial index measured by Doppler stethoscope <0.9. Subclinical stroke was defined by a medical history of a TIA without evidence on magnetic resonance imaging (MRI).

Participants were also administered the Center for Epidemiological Studies-Depression scale (CES-D; (20)) to assess depressive symptoms, but the CES-D was not included in the calculation of the multimorbidity index score.

PET Imaging

Annual resting-state cerebral blood flow (CBF) scans were acquired on a GE Advance PET scanner in 3-dimensional mode (image matrix = 128 × 128, 35 slices, voxel size = 2 × 2 mm, slice thickness = 4.25 mm) and reconstructed with a filtered back projection after a 10 mCi injection of ^{15}O -water. Images were obtained for 60 seconds once the total radioactivity counts in the brain reached threshold levels. A transmission scan in 2-dimensional mode using a ^{68}Ge rotating source was applied for attenuation correction. Using Statistical Parametric Mapping (SPM12 Wellcome Department of Cognitive Neurology, London, England), the PET scans were spatially normalized into standard stereotaxic space and smoothed using a gaussian kernel to a full width at half maximum of 10, 10, and 10 mm in the x, y, and z planes, respectively. To control for variability in global flow, rCBF at each voxel was ratio-adjusted to the mean global flow and scaled to 50 mL/100 g/min for each image.

PET Imaging Analysis

To examine the association between multimorbidity index score and brain function, whole brain voxel-wise multiple regression analyses were performed using statistical parametric mapping (SPM12),

controlling for baseline age and sex. Significant regions showing an association between multimorbidity index score and rCBF were identified using a magnitude threshold of $p \leq .005$, and a cluster size requirement of ≥ 50 contiguous voxels, as standardly used in BLSA PET studies (21–23). To control for potential effects of brain volume on rCBF, the analyses were repeated while controlling (covarying) for the MRI gray matter (GM) and white matter (WM) volume of each cluster observed in the PET analyses in a subsample who also had structural data ($n = 83$). To control for the effects of depressive symptoms on differences in rCBF, the analysis was also repeated using the continuous CES-D score as a covariate.

For each participant, the first available PET scan with a concurrent multimorbidity index score was used as the baseline scan. For the baseline analysis, the baseline rCBF was regressed on the baseline multimorbidity index scores, controlling for age and sex. To determine if individual health conditions contributed to the overall pattern related to multimorbidity, the conditions that make up the multimorbidity index score were individually analyzed to assess the contributions of each disease condition to the observed associations seen in the baseline index score model. To ensure a proper fit of these models, the analyses were limited to the 3 conditions with a prevalence $>20\%$ in the sample: hypertension, joint disease, and CKD. In these analyses, a mask of baseline regions exhibiting associations between index score and baseline rCBF was created. The effect of each condition on rCBF was then examined separately by regressing baseline rCBF on the individual condition scores, controlling for age and sex, limited to voxels within the masked regions from the baseline analysis ($p < .05$, $k = 50$ voxels).

In the longitudinal analysis, change in rCBF was examined as a function of change in multimorbidity score. For each participant with longitudinal multimorbidity data available at each PET assessment ($n = 74$), a slope CBF image was created that quantified the rate of change in CBF over time. For each voxel, a linear mixed effects model (fixed effect of time, random effects of intercept and slope) was implemented and the estimated random effects for slope were extracted. Change in multimorbidity was determined by calculating the difference between the first and last index score. The relationship between change in multimorbidity and voxel-wise change in rCBF and was then assessed using a multiple regression analysis, controlling for baseline age, sex, and longitudinal follow-up interval. To control for potential effects of change in brain volume on change in rCBF, the analyses were repeated while controlling for the rate of change in GM and WM volume of each cluster observed in the longitudinal PET analyses in a subsample who also had structural data ($n = 67$). In follow-up analyses, individual health conditions were assessed to determine contributions to the overall pattern related to increased multimorbidity. The conditions with the highest prevalence in the sample ($>20\%$) at last visit were again individually analyzed to assess the contributions of each disease condition to the observed associations seen in the longitudinal change model. In these analyses, a mask of longitudinal change in regions exhibiting associations between change in index score and change in rCBF was created. The effect of incidence of each medical condition at last visit on changes in rCBF was then examined separately, limited to voxels within the masked regions from the longitudinal analysis ($p < .05$, $k = 50$ voxels).

MRI Scanning

MRI structural images were acquired using either a GE Signa 1.5 T or Philips Achieva 3 T scanner. A 3-D T1-weighted spoiled gradient

refocused (SPGR) MRI scan (TR = 35 ms TR, TE = 5 ms, 8° flip angle, 256×256 matrix, 0.94×0.94 mm² voxel size, 1.5 mm slice thickness, 124 slices) was collected on the GE scanner, and a MPRAGE T1 scan was collected on the Philips scanner (TR = 6.8 ms, TE = 3.2 ms, 8° flip angle, 256×256 matrix, 1×1 mm² voxel size, 1.2 mm slice thickness, and 170 sagittal slices). Eighty-three of the 97 participants had MRI data available for use.

MRI GM and WM Volume Calculation

Volume data were extracted from RAVENS (Regional Analysis of Volumes Examined in Normalized Space) maps (24). The intensity values in a RAVENS map quantifies the regional distribution of GM, WM, and cerebrospinal fluid (CSF), with one RAVENS map for each tissue type. RAVENS values in the template space are directly proportional to the volume of the respective structures in the original brain scan.

In BLSA, to achieve optimal consistency between regional (volumetric) and voxel-wise analyses, we used a region of interest (ROI)-based segmentation approach in the calculation of RAVENS maps. To do this, anatomical ROIs were first segmented on the T1-weighted scan of each participant using a method that combines the MUSE anatomical labeling approach (25) with harmonized acquisition-specific atlases (26). The tissue type of each ROI was then used to segment the brain into GM, WM, and CSF. Also, to make the RAVENS calculation more robust to registration errors, we applied an “ensemble approach” by using 3 state-of-the-art deformable registration methods, DRAMMS (27), ANTS (28), and DEMONS (29), for subject-to-template warping, and by averaging RAVENS maps obtained using each method to compute the final RAVENS values.

Binary maps of the clusters showing an association between multimorbidity index score and CBF were generated from the PET analysis, and total volumes of GM + WM were calculated within each cluster for each participant. The clusters were corrected for intracranial volume (ICV) tissue volume and scanner strength (1.5 vs 3T), then included as a covariate in the follow-up PET analyses.

In the baseline PET analysis, the ICV-corrected tissue volume for each cluster was then included as a covariate in the follow-up PET analyses. In the longitudinal PET analysis, the rate of change in MRI volume of each cluster was included as a covariate in the follow-up analyses.

Results

Multimorbidity

Participants had a mean multimorbidity index score of 2.86 (1.63 SD) and a range of 0–7 conditions at baseline (Supplementary Figure 1). These scores were similar to those observed in a larger sample of BLSA participants (19). At baseline, hypertension ($n = 69$; 70%), joint disease ($n = 62$; 64%), and CKD ($n = 34$; 35%) were the most prevalent conditions in the sample, followed by diabetes, anemia, cancer, subclinical stroke, ischemic heart disease, and COPD. Hip fracture, congestive heart failure, peripheral artery disease, and Parkinson’s disease were the least prevalent conditions. At the last visit, participants had a mean multimorbidity index score of 3.24 (1.79 SD) and a range of 0–7 conditions. Overall, 44 participants had unchanged index scores over time, 18 participants increased by 1 condition, 10 participants increased by 2 conditions, and 2 participants increased by 3 conditions. Although only 30 of the 74 participants increased index score over time, there was a significant difference between first and last

visit scores for the group (paired sample *t*-test, $p < .001$). Hypertension (70%), joint disease (77%), and CKD (40%) were again the most prevalent conditions at the last assessment. While hypertension remained unchanged, there was a 13% increase in joint disease, 7% increase in subclinical stroke, and a 5% increase in COPD, CKD, and anemia over the follow-up interval. Parkinson's disease, congestive heart failure, and ischemic heart disease increased by 2%, followed by a 1% increase in diabetes.

PET Imaging

Baseline associations

The baseline multimorbidity index scores showed both negative and positive relationships with baseline rCBF ($n = 97$). Higher multimorbidity index score was related to lower rCBF in the right orbitofrontal cortex (Brodmann Area [BA] 11), superior frontal (BA 8, 10), and medial frontal cortices (BA 9). Higher multimorbidity index score was also related to lower rCBF in the right temporal pole (BA 38), and the left parahippocampal gyrus (BA 36). All regions remained significant when controlling for tissue volume of each cluster with the exception of the parahippocampal gyrus. These findings suggest that higher disease burden is related to lower brain activity, as measured by lower rCBF, in frontal and temporal brain regions.

Positive relationships, demonstrating higher rCBF in relation to higher multimorbidity index scores, were observed in the right middle temporal gyrus (BA 21), left inferior parietal cortex (BA 40), bilateral cuneus (BA 18), and cerebellum (Figure 1, Table 2). All regions remained significant when controlling for tissue volume of each cluster with the exception of the inferior parietal cortex. These findings suggest that higher disease burden also is associated with higher or preserved brain activity in posterior brain areas including temporal and occipital cortices.

Neither negative nor positive relationships between multimorbidity index score and rCBF changed when controlling for depressive symptoms as a continuous score. Additionally, no main effects of age or sex were observed in regions showing a relationship between multimorbidity and rCBF.

Baseline contributions of individual disease components

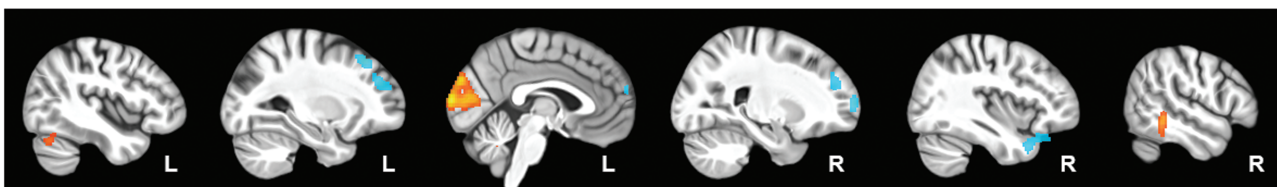
To help understand if individual disease conditions contribute to the overall patterns of rCBF differences seen with greater disease burden, rCBF in significant regions at baseline was regressed on the presence of specific disease conditions at baseline. The analyses were limited to the conditions with the highest prevalence in the sample ($>20\%$). When examining hypertension (HTN), joint disease, and CKD, HTN and CKD showed individual contributions to the altered patterns of blood flow. At baseline, both HTN and CKD were related to with lower rCBF in superior frontal cortices (BA 10), with CKD exhibiting additional associations with lower rCBF in temporal pole (BA 38) and parahippocampal gyrus (BA 36) regions. HTN and CKD were also related to with greater rCBF, with HTN associated with greater rCBF in the middle temporal gyrus (BA 21) and cuneus (BA 18), and CKD associated with greater rCBF in the cuneus (BA 18) and cerebellum (Figure 2, Table 3).

Longitudinal analysis

The longitudinal multimorbidity index scores showed mostly positive relationships with longitudinal change in rCBF ($n = 74$). Positive relationships, demonstrating increased rCBF in relation to increased multimorbidity index score, were observed in the left orbitofrontal cortex (BA 11), right basal forebrain, left middle temporal gyrus (BA 21), right paracentral gyrus (BA 20), bilateral brainstem, and left cerebellum (Figure 1, Table 2). Most regions remained significant when controlling for change in tissue volume of each cluster over time, except the basal forebrain region. This region was no longer significant at $p < .005$ when controlling for change in tissue volume, yet was observed at a lower threshold of $p < .05$. These findings suggest that increasing disease burden is associated with in increasing brain activity in predominately anterior cortical areas including frontal and temporal areas.

Increased multimorbidity index score was related to decreased rCBF in the left middle temporal gyrus (BA 21). This region remained significant when controlling for change in tissue volume. This finding suggests that increasing disease burden is related to relatively circumscribed decreases in brain activity over time.

Baseline Associations



Longitudinal Change

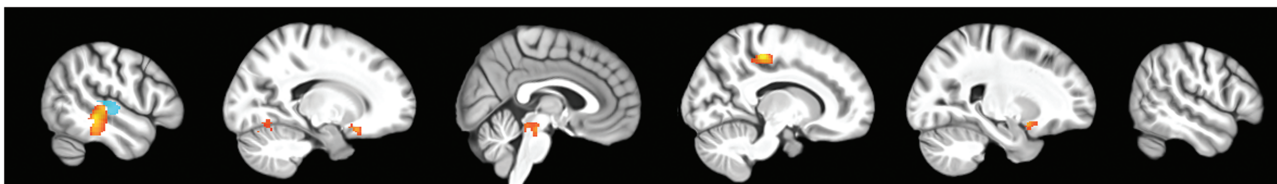


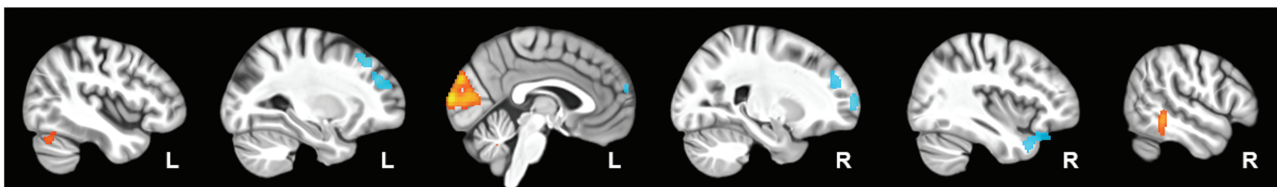
Figure 1. Multimorbidity and brain function. Regions where higher multimorbidity scores correlated with levels of brain activity measured by rCBF ($p < .005$, >50 voxels) are shown on sagittal slices beginning in the left and progressing through the right hemisphere. Regional patterns are shown at baseline and in longitudinal change over time. Blue represents regions of lower baseline or decreased longitudinal activity; orange represents regions of higher or increased activity.

Table 2. Associations Between Multimorbidity and Brain Activity

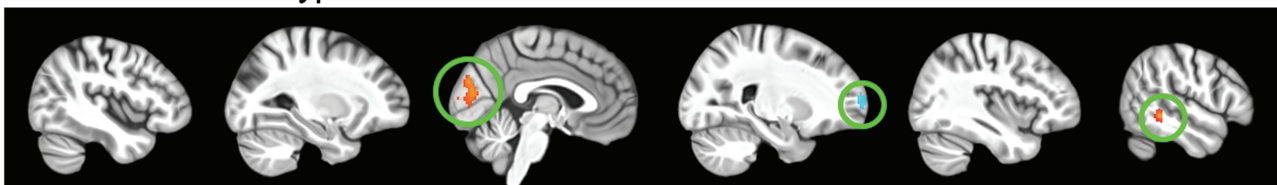
Region	Side	MNI Coordinate			Z score	p Value	voxels
		x	y	z			
<i>Baseline Visit</i>							
Lower Activity							
Orbitofrontal Cortex (11)	R	6	46	-28	3.01	.001	60
Superior Frontal Gyrus (10)	L	-8	68	8	3.40	<.001	95
Superior Frontal Gyrus (10)	R	26	64	8	4.09	<.001	175
Superior Frontal Gyrus (8)	L	-28	30	46	4.01	<.001	381
Superior Frontal Gyrus (8)	R	12	44	44	3.34	<.001	51
Medial Frontal Gyrus (9)	R	22	48	24	3.07	.001	80
Temporal Pole (38)	R	38	16	-32	3.19	.001	315
Parahippocampal Gyrus (36)	L	-14	-10	-34	3.49	<.001	121
Higher Activity							
Middle Temporal Gyrus (21)	R	52	-42	-8	3.38	<.001	143
Cuneus (18)	B	0	-100	10	4.40	<.001	974
Inferior Parietal Cortex (40)*	L	-30	-42	46	3.31	.001	50
Cerebellum	L	-46	-68	-26	3.37	.001	160
Cerebellum	R	4	-58	-32	3.10	<.001	109
<i>Longitudinal Change</i>							
Decreased Activity Over Time							
Middle Temporal Gyrus (21)	L	-54	-22	0	3.79		161
Increased Activity Over Time							
Orbitofrontal Cortex (11)	L	-18	16	-18	3.66	<.001	66
Basal Forebrain**	R	22	8	-14	3.73	<.001	56
Middle Temporal Gyrus (21)	L	-52	-32	-6	5.16	<.001	281
Paracentral Gyrus (20)	R	14	-30	50	4.64	<.001	147
Brainstem	B	2	-26	-18	3.55	<.001	76
Cerebellum	L	-16	-66	-14	3.09	.001	60

Note: Regions showing a relationship between multimorbidity score and brain activity measured by rCBF at baseline and change over time. The level of activity in relation to increasing multimorbidity score is noted. Stereotaxic coordinates are listed; Brodmann areas (BA) are indicated in parentheses. *denotes regions that did not survive tissue volume correction; **regions that did not survive tissue volume correction at $p < .005$, but were observed at $p < .05$.

Baseline Associations



Contributions of Hypertension



Contributions of Chronic Kidney Disease



Figure 2. Contributions of individual disease components at baseline. Of the 3 index components examined, hypertension and chronic kidney disease showed individual contributions to the multimorbidity pattern observed at baseline. Significant regional correlations are circled in green. Lower brain activity is indicated in blue, and higher activity in orange.

Table 3. Individual Disease Components and Brain Activity

Region	Side	MNI Coordinate			Z score	p value	Condition
		x	y	z			
<i>Baseline Associations</i>							
<i>Lower Activity</i>							
Superior Frontal Gyrus (10)	L	-4	62	22	3.29	<.001	CKD
Superior Frontal Gyrus (10)	R	26	62	12	2.88	.002	HTN
Superior Frontal Gyrus (8)	L	-24	28	44	2.94	.002	CKD
Temporal Pole (38)	R	34	12	-28	4.03	<.001	CKD
Parahippocampal Gyrus (36)	L	-8	-2	-26	3.09	.002	CKD
<i>Higher Activity</i>							
Middle Temporal Gyrus (21)	R	50	-42	-6	3.49	<.001	HTN
Cuneus (18)	L	-6	-82	18	2.60	.005	HTN
Cuneus (18)	B	-8	-100	22	3.28	.001	CKD
Cuneus (18)	R	6	-88	10	2.11	.017	CKD
Cerebellum	R	6	-52	-32	3.07	.001	CKD

Note: Regions where individual conditions contributed to the pattern of brain activity associated with multimorbidity score at baseline. Of the 3 index components examined, hypertension (HTN) and chronic kidney disease (CKD) showed individual contributions to the multimorbidity pattern observed at baseline. Stereotaxic coordinates are listed; Brodmann areas are indicated in parentheses.

Longitudinal contributions of individual disease components

When examining HTN, joint disease, and CKD in relation to changes in rCBF over time, no relationships were seen between increased incidence of these conditions and changes in rCBF. This is likely due to minor increases in the incidence of the conditions over time (HTN incidence unchanged; joint disease 13% increase; CKD 5% increase over time).

Discussion

Using data from participants in the Baltimore Longitudinal study of Aging, our results show that disease burden is associated with brain function in older individuals. Greater disease burden was related to both lower and higher relative brain activity as measured by rCBF. At baseline, greater multimorbidity was associated with lower rCBF in frontal and anterior temporal lobe regions, and with higher rCBF in middle temporal, parietal and occipital areas of the brain. Over time, increasing multimorbidity scores were related to decreased rCBF in lateral temporal cortex and increased rCBF and frontal and temporal lobe areas. These findings demonstrate that physical health, often primarily associated with dysfunction of other organ systems in the body, is associated with altered functional patterns in the aging brain.

At baseline, participants in this sample had an average of 2.86 disease conditions, with a range of 0–7 conditions among the 13 used to construct the multimorbidity index score. Hypertension, joint disease and CKD were the most prevalent conditions, followed by diabetes, anemia, cancer, and subclinical stroke. At the last visit approximately 5 years later, the multimorbidity index score increased to an average of 3.24 disease conditions, with hypertension, joint disease, and CKD remaining the most prevalent conditions. These findings support other studies of disease prevalence in aging (30,31).

With regard to brain function, higher multimorbidity was associated with lower rCBF at baseline in the frontal lobes of the brain including orbitofrontal and superior frontal regions. Other areas of lower rCBF were seen in the temporal pole and parahippocampal gyrus. Several regions also exhibited higher relative rCBF in relation to higher multimorbidity index scores at baseline. Higher rCBF was seen in lateral temporal, occipital, parietal, and cerebellar regions. Longitudinally, we found decreased rCBF over time observed in the

middle temporal gyrus and increased rCBF observed in orbitofrontal, basal forebrain, middle temporal, brainstem, and cerebellar regions in relation to increasing multimorbidity scores over time. As some of these longitudinal changes were observed in areas contralateral to those seen at baseline, it is conceivable that these represent some form of compensatory activity in response to the differences in baseline activity.

Together, these results show that greater multimorbidity is associated with widespread areas of lower brain activity, supporting a link between health and decreases in aging brain function. As for increased activity, increased brain activity in aging has historically been interpreted as compensatory in nature, with the theory that increased activity in some areas may compensate for decreased activity in others (32,33). More recent theories, however, suggest that increased activity might also represent an excitotoxic reaction to increasing neuropathology in aging (34,35), or represent a failure to properly inhibit activity levels (36) with increasing age-related neuropathologic burden. Alternately, higher relative rCBF in some regions may reflect an attempt at preservation of function in view of age-related declines in global cerebral blood flow.

Vascular issues related to disease states may also play a role in the increased rCBF observed here. Health conditions can result in compromised vascular autoregulation and neurovascular coupling (37). While vascular dysregulation is typically presumed to result in decreased cerebral blood flow, recent evidence suggests that there are bidirectional effects on neuronal firing in the brain. Indeed, Kim et al. (38) propose that there are “vasculo-neuronal” coupling effects that can lead to both decreased and increased neuronal activity in relation to changes in vascular tone, with increased neuronal firing also occurring in response to decreased tissue perfusion. Additionally, studies of hypertension (39), impaired insulin resistance (40), and anemia (41) have found increased brain activity in relation to disease. Although it is difficult to define the underlying causes of the observed associations, both higher and lower rCBF in relation to greater disease burden indicate that poorer health results in altered brain function in aging.

Because the multimorbidity index score represents a compilation of multiple health conditions, we also examined the role of individual conditions in the overall pattern of compromised rCBF. Of the most common health conditions occurring in this

group, hypertension and CKD showed individual contributions at baseline. These differences were seen in frontal, temporal, and occipital regions, and support previous studies illustrating functional alterations associated with hypertension (22,42). Although little is known regarding brain activity in CKD in humans, it has recently been shown that CKD results in decreased acetylcholinesterase activity in the brain, as well as dendritic spine loss in the cerebral cortex and hippocampus in mice (43), which could contribute to the associations observed here. Taken together, however, the findings also show that no single illness explains the overall pattern associated with multimorbidity. This suggests that combinations of conditions may have synergistic effects on brain function, perhaps through a commonly shared pathway such as inflammation or vascular dysregulation, which can result from a number of health-related conditions, and are also strong predictors of multimorbidity (44). The high prevalence of certain conditions in our sample, however, suggests that hypertension, joint disease, and CKD likely provide the greatest contribution to the relationship between multimorbidity and brain function observed in this study.

Although cerebral blood flow was measured during the resting state, the activity patterns are of interest, as many of these areas are associated with higher order cognitive function. For example, the orbitofrontal cortex is associated with planning, decision making and judgment, memory, and emotion (45,46), the superior frontal cortex is associated with memory, executive function, and spatial processing (47,48), and the temporal pole is associated with memory, semantic processes, and the conceptualization of object properties (49). The middle temporal gyrus is part of the ventral visual pathway which is associated with memory and visual perception (50,51) and is also involved in language processes (52), and the cuneus is another a crucial component of the ventral visual pathway. Although our participants remained cognitively normal throughout the study interval, the correlation between multimorbidity and rCBF suggests that frontal, temporal and occipital areas may be more vulnerable to altered function with increased disease burden.

These patterns of altered rCBF add to our knowledge about the relationship between disease and brain function in aging. Previous studies have suggested that multimorbidity may play a role in structural and functional alterations, particularly in brain regions vulnerable to neuropathologic changes in AD (12,13). Although we did not restrict our analysis to specific regions of the brain, we found that multimorbidity is associated with altered function of frontal, and temporal regions which are sites of early pathological change in AD (53,54), and include the regions previously associated with multimorbidity (12). These frontal, temporal, and occipital regions are also important for their role in memory and perceptual processes.

One limitation of our study is the absence of a measure of disease severity for the conditions that compose the multimorbidity index score. Although BLSA participants are aware of their health conditions and pursue treatment when warranted, severity of illness would certainly play a role in quality of life and might also be a factor in the effect of illness on brain function in the older population. Additionally, WM hyperintensity volumes would have been a useful measure of cerebrovascular disease associated with multimorbidity, but our current analyses include both 1.5 and 3T data which used different imaging protocols that detect WM lesions. While efforts are ongoing to harmonize lesions measured from these different image acquisitions, these data are not yet available in the present

study. Finally, the follow-up interval for the longitudinal analysis was relatively short and additional relationships may emerge over longer intervals, and with a larger proportion of the sample exhibiting increased multimorbidity scores over time.

Together, our results show that multimorbidity affects brain function in older individuals, and that hypertension and CKD play individual roles in the altered patterns of activity. The decreased activity in frontal and temporal lobe areas is particularly notable due to their role in memory, planning, decision making, and emotion. Altered activity in these areas raises the possibility of planning and decision making vulnerability with increased disease burden in the future, at a time when these processes may be crucial for making proper health care decisions that can greatly impact quality of life. It is also equally important to note that many of the health conditions commonly observed in aging are modifiable with treatment and lifestyle changes, which may reduce the impact of multimorbidity on the brain. Thus, maximizing health and preventing multimorbidity should be a primary goal in the care and treatment of the older population to preserve both physical and brain function.

Supplementary Material

Supplementary data are available at *The Journals of Gerontology, Series A: Biological Sciences and Medical Sciences* online.

Acknowledgments

We are grateful to the BLSA participants and staff for their dedication to these studies and the staff of The Johns Hopkins PET facility, the Wong lab fellows, and staff at The Johns Hopkins University and Hospital for their assistance. We dedicate this report to the memory of our friend, colleague, and co-author Chiung-Wei Huang. Her outstanding skills, positive outlook, and steady support were critical for this work and are greatly missed.

Funding

This research was supported by the Intramural Research Program of the National Institutes of Health, National Institute on Aging.

Conflict of Interest

None declared.

References

- Niccoli T, Partridge L. Ageing as a risk factor for disease. *Curr Biol*. 2012;22(17):R741–R752. doi:10.1016/j.cub.2012.07.024
- Gerteis J, Izrae ID, Deitz D, et al. *Multiple Chronic Conditions Chartbook*. vol Q14-0038. AHRQ Publications. Agency for Healthcare Research and Quality, Rockville, MD; 2014.
- The State of Aging and Health in America 2013. *US Dept of Health and Human Service*; 2013.
- Keefover RW. Aging and cognition. *Neurol Clin*. 1998;16(3):635–648. doi:10.1016/s0733-8619(05)70085-2
- Schönknecht P, Pantel J, Kruse A, Schröder J. Prevalence and natural course of aging-associated cognitive decline in a population-based sample of young-old subjects. *Am J Psychiatry*. 2005;162(11):2071–2077. doi:10.1176/appi.ajp.162.11.2071
- Oosterveld SM, Kessels RP, Hamel R, et al. The influence of co-morbidity and frailty on the clinical manifestation of patients with Alzheimer's disease. *J Alzheimers Dis*. 2014;42(2):501–509. doi:10.3233/JAD-140138
- Vassilaki M, Aakre JA, Cha RH, et al. Multimorbidity and risk of mild cognitive impairment. *J Am Geriatr Soc*. 2015;63(9):1783–1790. doi:10.1111/jgs.13612

8. Roberts RO, Cha RH, Mielke MM, et al. Risk and protective factors for cognitive impairment in persons aged 85 years and older. *Neurology*. 2015;84(18):1854–1861. doi:10.1212/WNL.0000000000001537
9. Grande G, Cucumo V, Cova I, et al. Reversible mild cognitive impairment: the role of comorbidities at baseline evaluation. *J Alzheimers Dis*. 2016;51(1):57–67. doi:10.3233/JAD-150786
10. Aubert L, Pichiéri S, Hommet C, Camus V, Berrut G, de Decker L. Association between comorbidity burden and rapid cognitive decline in individuals with mild to moderate Alzheimer's disease. *J Am Geriatr Soc*. 2015;63(3):543–547. doi:10.1111/jgs.13314
11. Solomon A, Dobranici L, Kåreholt I, Tudose C, Lăzărescu M. Comorbidity and the rate of cognitive decline in patients with Alzheimer dementia. *Int J Geriatr Psychiatry*. 2011;26(12):1244–1251. doi:10.1002/gps.2670
12. Vassilaki M, Aakre JA, Mielke MM, et al. Multimorbidity and neuroimaging biomarkers among cognitively normal persons. *Neurology*. 2016;86(22):2077–2084. doi:10.1212/WNL.0000000000002624
13. King KS, Peshock RM, Rossetti HC, et al. Effect of normal aging versus hypertension, abnormal body mass index, and diabetes mellitus on white matter hyperintensity volume. *Stroke*. 2014;45(1):255–257. doi:10.1161/STROKEAHA.113.003602
14. Jueptner M, Weiller C. Review: does measurement of regional cerebral blood flow reflect synaptic activity? Implications for PET and fMRI. *Neuroimage*. 1995;2(2):148–156. doi:10.1006/nimg.1995.1017
15. Cherry SR, Phelps ME. Imaging brain function with positron emission tomography. In: Toga AW, Mazziotta JC, eds. *Brain Mapping, The Methods*. Academic Press; 1996:191–221.
16. Fabbri E, Zoli M, Gonzalez-Freire M, Salive ME, Studenski SA, Ferrucci L. Aging and multimorbidity: new tasks, priorities, and frontiers for integrated gerontological and clinical research. *J Am Med Dir Assoc*. 2015;16(8):640–647. doi:10.1016/j.jamda.2015.03.013
17. Stone JL, Norris AH. Activities and attitudes of participants in the Baltimore longitudinal study. *J Gerontol*. 1966;21(4):575–580. doi:10.1093/geronj/21.4.575
18. Fabbri E, An Y, Zoli M, et al. Aging and the burden of multimorbidity: associations with inflammatory and anabolic hormonal biomarkers. *J Gerontol A Biol Sci Med Sci*. 2015;70(1):63–70. doi:10.1093/geron/glu127
19. Fabbri E, An Y, Zoli M, et al. Association between accelerated multimorbidity and age-related cognitive decline in older Baltimore longitudinal study of aging participants without dementia. *J Am Geriatr Soc*. 2016;64(5):965–972. doi:10.1111/jgs.14092
20. Radloff LS. The CES-D scale: a self-report depression scale for research in the general population. *Applied Psychol Measurement*. 1977;1(1):385–401. doi:10.1177/014662167700100306
21. Beason-Held LL, Kraut MA, Resnick SM. I. Longitudinal changes in aging brain function. *Neurobiol Aging*. 2008;29(4):483–496. doi:10.1016/j.neurobiolaging.2006.10.031
22. Beason-Held LL, Moghekar A, Zonderman AB, Kraut MA, Resnick SM. Longitudinal changes in cerebral blood flow in the older hypertensive brain. *Stroke*. 2007;38(6):1766–1773. doi:10.1161/STROKEAHA.106.477109
23. Beason-Held LL, Goh JO, An Y, et al. Changes in brain function occur years before the onset of cognitive impairment. *J Neurosci*. 2013;33(46):18008–18014. doi:10.1523/JNEUROSCI.1402-13.2013
24. Davatzikos C, Genc A, Xu D, Resnick SM. Voxel-based morphometry using the RAVENS maps: methods and validation using simulated longitudinal atrophy. *Neuroimage*. 2001;14(6):1361–1369. doi:10.1006/nimg.2001.0937
25. Doshi J, Erus G, Ou Y, et al.; Alzheimer's Neuroimaging Initiative. MUSE: Multi-atlas region Segmentation utilizing Ensembles of registration algorithms and parameters, and locally optimal atlas selection. *Neuroimage*. 2016;127:186–195. doi:10.1016/j.neuroimage.2015.11.073
26. Erus G, Doshi J, An Y, Verganelakis D, Resnick SM, Davatzikos C. Longitudinally and inter-site consistent multi-atlas based parcellation of brain anatomy using harmonized atlases. *Neuroimage*. 2018;166:71–78. doi:10.1016/j.neuroimage.2017.10.026
27. Ou Y, Sotiras A, Paragios N, Davatzikos C. DRAMMS: deformable registration via attribute matching and mutual-saliency weighting. *Med Image Anal*. 2011;15(4):622–639. doi:10.1016/j.media.2010.07.002
28. Avants B, Duda JT, Kim J, et al. Multivariate analysis of structural and diffusion imaging in traumatic brain injury. *Acad Radiol*. 2008;15(11):1360–1375. doi:10.1016/j.acra.2008.07.007
29. Yeo BT, Sabuncu MR, Vercauteren T, Ayache N, Fischl B, Golland P. Spherical demons: fast diffeomorphic landmark-free surface registration. *IEEE Trans Med Imaging*. 2010;29(3):650–668. doi:10.1109/TMI.2009.2030797
30. Marengoni A, Rizzuto D, Wang HX, Winblad B, Fratiglioni L. Patterns of chronic multimorbidity in the elderly population. *J Am Geriatr Soc*. 2009;57(2):225–230. doi:10.1111/j.1532-5415.2008.02109.x
31. Salive ME. Multimorbidity in older adults. *Epidemiol Rev*. 2013;35:75–83. doi:10.1093/epirev/mxs009
32. Grady CL, McIntosh AR, Rajah MN, Beig S, Craik FI. The effects of age on the neural correlates of episodic encoding. *Cereb Cortex*. 1999;9(8):805–814. doi:10.1093/cercor/9.8.805
33. Madden DJ, Gottlob LR, Allen PA. Adult age differences in visual search accuracy: attentional guidance and target detectability. *Psychol Aging*. 1999;14(4):683–694. doi:10.1037/0882-7974.14.4.683
34. Sojkova J, Beason-Held L, Zhou Y, et al. Longitudinal cerebral blood flow and amyloid deposition: an emerging pattern? *J Nucl Med*. 2008;49(9):1465–1471. doi:10.2967/jnumed.108.051946
35. Sperling RA, Laviolette PS, O'Keefe K, et al. Amyloid deposition is associated with impaired default network function in older persons without dementia. *Neuron*. 2009;63(2):178–188. doi:10.1016/j.neuron.2009.07.003
36. Andrews-Zwilling Y, Bien-Ly N, Xu Q, et al. Apolipoprotein E4 causes age- and Tau-dependent impairment of GABAergic interneurons, leading to learning and memory deficits in mice. *J Neurosci*. 2010;30(41):13707–13717. doi:10.1523/JNEUROSCI.4040-10.2010
37. Coucha M, Abdelsaid M, Ward R, Abdul Y, Ergul A. Impact of metabolic diseases on cerebral circulation: structural and functional consequences. *Compr Physiol*. 2018;8(2):773–799. doi:10.1002/cphy.c170019
38. Kim KJ, Ramiro Diaz J, Iddings JA, Filosa JA. Vasculo-neuronal coupling: retrograde vascular communication to brain neurons. *J Neurosci*. 2016;36(50):12624–12639. doi:10.1523/JNEUROSCI.1300-16.2016
39. Jennings JR, Muldoon MF, Ryan C, et al. Reduced cerebral blood flow response and compensation among patients with untreated hypertension. *Neurology*. 2005;64(8):1358–1365. doi:10.1212/01.WNL.0000158283.28251.3C
40. Thambisetty M, Beason-Held LL, An Y, et al. Impaired glucose tolerance in midlife and longitudinal changes in brain function during aging. *Neurobiol Aging*. 2013;34(10):2271–2276. doi:10.1016/j.neurobiolaging.2013.03.025
41. Gottesman RF, Sojkova J, Beason-Held LL, et al. Patterns of regional cerebral blood flow associated with low hemoglobin in the Baltimore Longitudinal Study of Aging. *J Gerontol A Biol Sci Med Sci*. 2012;67(9):963–969. doi:10.1093/geron/gls121
42. Dai W, Lopez OL, Carmichael OT, Becker JT, Kuller LH, Gach HM. Abnormal regional cerebral blood flow in cognitively normal elderly subjects with hypertension. *Stroke*. 2008;39(2):349–354. doi:10.1161/STROKEAHA.107.495457
43. Mazumder MK, Paul R, Bhattacharya P, Borah A. Neurological sequel of chronic kidney disease: from diminished Acetylcholinesterase activity to mitochondrial dysfunctions, oxidative stress and inflammation in mice brain. *Sci Rep*. 2019;9(1):3097. doi:10.1038/s41598-018-37935-3
44. Bektas A, Schurman SH, Sen R, Ferrucci L. Aging, inflammation and the environment. *Exp Gerontol*. 2018;105:10–18. doi:10.1016/j.exger.2017.12.015
45. Bechara A, Damasio H, Damasio AR. Emotion, decision making and the orbitofrontal cortex. *Cereb Cortex*. 2000;10(3):295–307. doi:10.1093/cercor/10.3.295
46. Frey S, Petrides M. Orbitofrontal cortex and memory formation. *Neuron*. 2002;36(1):171–176. doi:10.1016/s0896-6273(02)00901-7
47. Cabeza R, Nyberg L. Imaging cognition II: an empirical review of 275 PET and fMRI studies. *J Cogn Neurosci*. 2000;12(1):1–47. doi:10.1162/08989290051137585
48. du Boisgueheneuc F, Levy R, Volle E, et al. Functions of the left superior frontal gyrus in humans: a lesion study. *Brain*. 2006;129(Pt 12):3315–3328. doi:10.1093/brain/awl244

49. Bonner MF, Price AR. Where is the anterior temporal lobe and what does it do? *J Neurosci*. 2013;33(10):4213–4215. doi:10.1523/JNEUROSCI.0041-13.2013
50. Grill-Spector K. The neural basis of object perception. *Curr Opin Neurobiol*. 2003;13(2):159–166. doi:10.1016/s0959-4388(03)00040-0
51. Ungerleider LG, Mishkin M. Two cortical visual systems. In: Ingle DJ, Goodale MA, Mansfield RJW, eds. *Analysis of Visual Behavior*. MIT Press; 1982:549–86.
52. Spitsyna G, Warren JE, Scott SK, Turkheimer FE, Wise RJ. Converging language streams in the human temporal lobe. *J Neurosci*. 2006;26(28):7328–7336. doi:10.1523/JNEUROSCI.0559-06.2006
53. Braak H, Braak E. Neuropathological staging of Alzheimer-related changes. *Acta Neuropathol*. 1991;82(4):239–259. doi:10.1007/BF00308809
54. Braak H, Braak E. Staging of Alzheimer's disease-related neurofibrillary changes. *Neurobiol Aging*. 1995;16(3):271–8; discussion 278. doi:10.1016/0197-4580(95)00021-6